High-resolution mapping of the optical near-field components at a triangular nano-aperture

D. Molenda[1], G. Colas des Francs[2], U.C. Fischer[1], N. Rau[3], and A. Naber[3]

[1] *Physikalisches Institut, Universität Münster, Wilhelm-Klemm-Str. 10, D-48149 Münster, Germany*

[2] *Laboratoire de Physique (LPUB-CNRS), Université de Bourgogne, 9, av. A. Savary, BP 47870, F-21078 Dijon cedex, France*

[3] *Institut für Angewandte Physik, Universität Karlsruhe (TH), Wolfgang-Gaede-Str. 1, D-76131 Karlsruhe, Germany*
andreas.naber@physik.uni-karlsruhe.de

Abstract: A triangular nano-aperture in an aluminum film was used as a probe in a scanning near-field optical microscope (SNOM) to image single fluorescent molecules with an optical resolution down to 30 nm. The differently oriented molecules were employed as point detectors to map the vectorial components of the electric field distribution at the illuminated triangular aperture. The good agreement of the experimental results with numerical simulations enabled us to determine both the field map at a triangular aperture and the exact orientations of the probing molecules.

OCIS codes: (180.5810) Scanning microscopy; (180.2520) Fluorescence microscopy; (050.1220) Apertures; (050.1960) Diffraction theory; (999.9999) Nano-optics

References and links

1. For a recent review, see B. Hecht, "Nano-optics with single quantum systems," Phil. Trans. R. Soc. Lond. A **362**, 881-899 (2004).
2. A. Dereux, C. Girard, and J.C. Weeber, "Theoretical principles of near-field optical microscopies and spectroscopies," J. Chem. Phys. **112**, 7775 (2000).
3. S. Linden, U. Neuberth, N. Rau, A. Naber, M. Wegener, S. Pereira, K. Busch, A. Christ, and J. Kuhl, "Near-field optical microscopy and spectroscopy of one-dimensional metallic photonic crystal slabs," Phys. Rev. B **71**, 245119 (2005).
4. E. Betzig and R. Chichester, "Single Molecules Observed by Near-Field Scanning Optical Microscopy," Science **262**, 1422 (1993).
5. J.A. Veerman, M.F. Garcia-Parajo, L. Kuipers, and N.F. van Hulst, "Single molecule mapping of the optical field distribution of probes for near-field microscopy," J. Microsc. **194**, 477 (1999).
6. H.G. Frey, S. Witt, K. Felderer, and R. Guckenberger, "High-Resolution Imaging of Single Fluorescent Molecules with the Optical Near-Field of a Metal Tip," Phys. Rev. Lett. **93**, 200801 (2004).
7. J. Koglin, U.C. Fischer, and H. Fuchs, "Material contrast in scanning near-field optical microscopy at 1–10 nm resolution," Phys. Rev. B **55**, 7977 (1997).
8. A. Naber, D. Molenda, U.C. Fischer, H.J. Maas, C. Höppener, N. Lu, and H. Fuchs, "Enhanced Light Confinement in a Near-Field Optical Probe with a Triangular Aperture," Phys. Rev. Lett. **89**, 210801 (2002).
9. J.A. Veerman, A.M. Otter, L. Kuipers, and N.F. van Hulst, "High definition aperture probes for near-field optical microscopy fabricated by focused ion beam milling," Appl. Phys. Lett. **72**, 3115 (1998).
10. G. Colas des Francs, D. Molenda, U.C. Fischer, and A. Naber, "Enhanced light confinement in a triangular aperture: Experimental evidence and numerical calculations," Phys. Rev. B **72**, 165111-6 (2005).
11. E. Bortchagovsky, G. Colas des Francs, D. Molenda, A. Naber, and U.C. Fischer, "On the confinement of the electric near field at optically excited triangular apertures in a metal film" (submitted).
12. K. Tanaka and M. Tanaka, "Analysis and numerical computation of diffraction of an optical field by a sub-wavelength-size aperture in a thick metallic screen by use of a volume integral equation," Appl. Opt. **43**, 1734 (2004).
13. F. de Lange, A. Cambi, R. Huijbens, B. de Bakker, W. Rensen, M. Garcia-Parajo, N.F. van Hulst, and C.G. Figdor, "Cell biology beyond the diffraction limit: near-field scanning optical microscopy," J. Cell Science **114**, 4153-60 (2001).

#9720 - $15.00 USD Received 23 November 2005; revised 15 December 2005; accepted 16 December 2005

14. M. Koopman, A. Cambi, B.I. de Bakker, B. Joosten, C.G. Figdor, N.F. van Hulst, and M.F. Garcia-Parajo, "Near-field scanning optical microscopy in liquid for high resolution single molecule detection on dendritic cells," FEBS Lett. **573**, 6-10 (2004).
15. C. Höppener, J.P. Siebrasse, R. Peters, U. Kubitscheck, and A. Naber, "High-Resolution Near-Field Optical Imaging of Single Nuclear Pore Complexes under Physiological Conditions," Biophys. J. **88**, 3681-8 (2005).

1. Introduction

Optical properties of single metallic or non-metallic nanostructures are still mainly investigated by classical methods like absorption and transmission measurements of light. Spatial information on a scale larger than half the wavelength of light ($\lambda/2$) can be easily obtained using conventional far-field optical microscopy techniques. The intensity distribution of the electromagnetic fields in the immediate vicinity of nanostructures, however, can only be deduced from near-field optical methods since the information contained in the evanescent fields around such structures are not transferred to the far-field [1].

The usual way to measure an optical near-field is to scan a submicroscopic detector several nanometers over the sample such that probe and sample can interact with each other via evanescent fields. The achievable optical resolution is mainly limited by the size of the detector and its distance to the sample. In a photon scanning tunneling microscope (PSTM), for example, the sharp tip of a tapered optical glass fiber or a submicroscopic aperture at the very end of a metal-coated glass fiber are employed as detectors for the near-field. The interpretation of a PSTM measurement, however, can be rather complicated because the influence of the probe on the field map as well as the special characteristics of the probe as detector for different electric and magnetic field components have to be taken into account [2,3].

A very effective method to determine the field map of an illuminated metallic nanostructure with molecular resolution was found by Betzig and Chichester in the context of the first single molecule fluorescence measurements at room temperature [4]. The fluorescence of single molecules embedded in a thin film of polymer was locally excited through a circular, 100-nm-sized aperture of a near-field probe and collected by an optical microscope. By scanning the aperture at a distance of 10 nm over a molecule, the intensity of the resulting fluorescence was modulated according to the varying local electric field intensity of the extended field distribution around the aperture. Thus, the measured fluorescence image corresponded to an intensity map of the electric field in the fixed direction of the molecular dipole transition 10 nm below the aperture. By comparing the field map with results of a well known theoretical model it was possible to roughly determine the orientation of a molecule within the polymer film. So far, similar measurements could be accomplished only for apertures sizes $d > 70$ nm and were carried out exclusively with circular apertures [4,5]. Recently, such a method was also used to characterize the electric field emitted by a *tip-on-aperture* [6].

In this paper, the electric field map at a 50-nm-sized triangular aperture (TA) in a metallic film is revealed using single molecule fluorescence measurements in combination with a numerical model. The excellent agreement of experimentally obtained field maps with results of the numerical simulation allowed us to determine with high accuracy the vectorial field components at a triangular aperture as well as the orientation of the measured molecules. Vice versa, we are able to demonstrate that a triangular aperture as near-field optical probe (TA probe) makes it possible to detect single fluorescent molecules with an optical resolution down to 30 nm. The high signal-to-noise ratio enabled us to localize a molecule within a few nanometers on a time scale of 20 ms.

2. Background and experimental details

Our method to form a triangular nano-aperture is based on a tetrahedral glass body which is simply fabricated by scratching and cleaving of a cover glass [7]. The common tip of three

#9720 - $15.00 USD Received 23 November 2005; revised 15 December 2005; accepted 16 December 2005

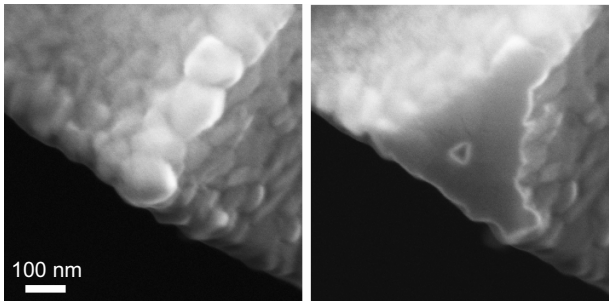

Fig. 1. Electron micrographs of an aluminum-coated tetrahedral glass tip before (left) and after (right) focused ion beam milling. Cutting off the metal-coated, ultra-sharp glass tip routinely results in a well-shaped triangular nano-aperture embedded in a flat aluminum end face.

orthogonal cleavage edges is known to be extraordinarily sharp which enables us to create TAs with sizes in the 10-nm-regime. After coating the glass tip with an opaque film of aluminum, an almost equilateral TA was formed either by gently squeezing the metal-coated tetrahedral tip against a flat glass surface [8] or by side-milling using a focused ion beam [9] (Fig. 1). The aperture is illuminated through the glass body along the direction of symmetry by means of a focused laser beam (wavelength λ=633 nm). Recently, such a TA was used as near-field probe for imaging quantum dot aggregates with an optical resolution of 30-40 nm [8]. Owing to the large opening angle of the glass tip, a TA probe proved to have an optical transmission coefficient several orders higher than conventional SNOM aperture probes based on thermally pulled fiber tips.

Previously, we have used single 20-nm-sized polysterene beads doped with a large number of differently oriented fluorescent molecules to map the optical near-field of a TA probe [8]. Due to the isotropic absorption properties of such beads, however, only the scalar intensity distribution could be measured. The results of a numerical simulation based on the field susceptibility technique were shown to be in good agreement to the experimental results though only a simplified model of an aperture in a planar film was used for the calculations [10].

To illuminate the unique electromagnetic properties of a TA, the calculated field maps of a circular aperture and a TA are compared in Fig. 2. Instead of two intensity maxima as in the case of a circular aperture, the electric field distribution at a TA is mainly confined to one side if the TA is illuminated with light of a polarization directed perpendicular to one of the three edges. For a polarization direction parallel to an edge, however, a field map is created which corresponds qualitatively to the one of a circular aperture (not shown) [8,10].

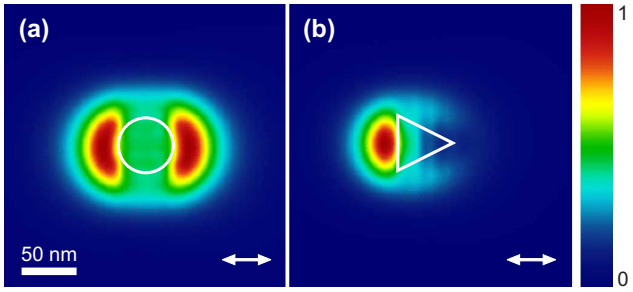

Fig. 2. Scalar electric field intensity calculated near a circular (a) and a triangular nano-aperture (b). The aluminum slab (thickness d=100 nm) separates a glass and an air half-space; the aperture is filled with glass. For the simulation, the aperture is assumed to be illuminated from the glass side by a monochromatic plane wave (λ=633 nm) which is linearly polarized parallel to the slab (white arrows). The intensity map is calculated at the air side in a plane 10 nm below the film (see also Fig. 5(a)). Intensities are normalized to the respective maximum values.

#9720 - $15.00 USD Received 23 November 2005; revised 15 December 2005; accepted 16 December 2005

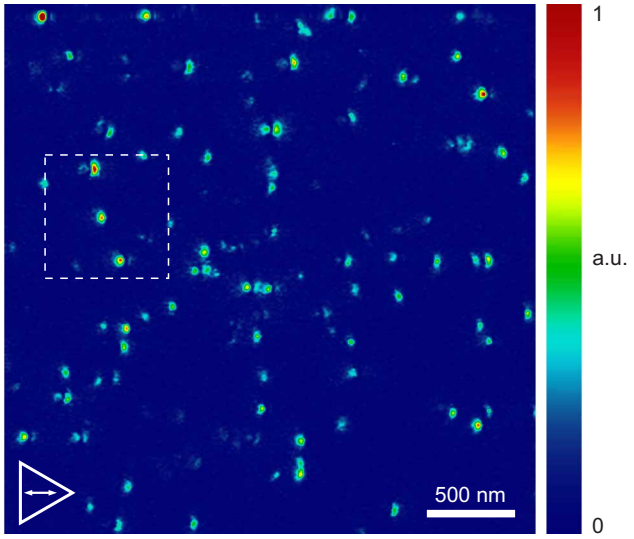

Fig. 3. Near-field optical fluorescence image of randomly oriented TDI molecules embedded in a 10-nm-thin PMMA film. The molecules are excited by means of a triangular aperture probe. The aperture is aligned relative to the sample as indicated by the white triangle. The white double-arrow represents the incident beam polarization. For an enlarged view of the framed area, see Fig. 4.

The major aim of this work was to measure the vectorial components of the electric field map at a TA by making use of differently oriented single molecules as detectors and to compare the experimental results with numerical calculations from our theoretical model. For this purpose, terrylenediimide (TDI) molecules were embedded in a 10-nm-film of polymethylmetacrylate (PMMA) by spin-coating an appropriate solution of TDI/PMMA/toluol on a clean cover slide. Our measurements described below indicate that under ambient conditions the spatial orientation of the TDI molecules in the PMMA film seems to be frozen to an arbitrary direction. Mainly as a result of the finite thickness of the PMMA film, the distance of the molecules to the TA ranges from 10 nm to 20 nm.

Fluorescence excitation of the molecules occurred through the near-field of the aperture which was illuminated by focused laser light (λ=633 nm) with a typical power of 1mW. The fluorescence light was collected by a 1.3-numerical-aperture oil-immersion-objective and was detected by an avalanche photo diode after passing a filter combination to suppress the excitation light (for more details, see Ref. 8).

3. Experimental results

Figure 3 displays a fluorescence image of TDI molecules in PMMA taken by a TA probe with a 50-nm-sized optical aperture. The image covers an area of 3µm x 3µm in which ~100 fluorescence spots of varying shape and intensity appear. Each of these patterns is interpreted as near-field map of a triangular aperture probed by a single, arbitrarily oriented molecule. The signal-to-noise (S/N) ratio of the intense spots is in the range of 20-30 (pixel time of 20 ms) and thus clearly higher than in comparable studies using fiber probes with larger apertures. Since the TA probe turned out to withstand laser intensities of > 50 mW, the S/N ratio may even be further improved easily. The distinct improvement of S/N ratio originates from the special geometry of a TA probe: first, the large taper angle of ~90° provides a relatively high transmission of light; and second, the excitation light is focused directly to the aperture through an only 0.5 mm long piece of glass thus avoiding unwanted background, for example, from a light-guiding fiber.

The fluorescence spots appearing in the image can be roughly classified in two categories: about half of the spots are composed of two sub-spots of different shape and intensity with a

#9720 - $15.00 USD Received 23 November 2005; revised 15 December 2005; accepted 16 December 2005

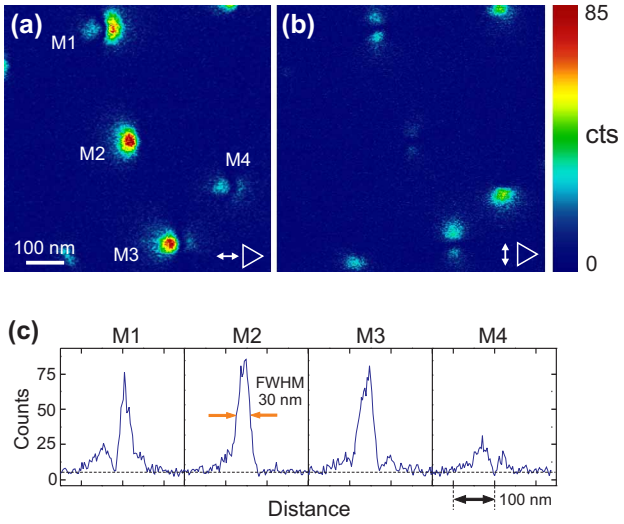

Fig. 4. (a,b) Enlarged view of the framed sample area in Fig. 3 for two different polarization directions of the incident light (indicated by double-arrows). As a result of the polarization rotation the intensity maximum and distribution of the fluorescence spots drastically changed. The different shape of the spots within an image is caused by different orientations of single molecules and represents a map of the electric field component at the triangular aperture in direction of the molecular dipole. Integration time per pixel was 20 ms. (c) Cross-sections along polarization direction through the center of the fluorescence spots M1-M4 in (a).

total extension of > 50 nm whereas the other half are mainly bright single spots with a size of 30-40 nm. A more detailed view of several different field maps produced by differently oriented molecules is presented in Fig. 4. The images Fig. 4(a) and 4(b) display exactly the same area of the sample, only the polarization direction of the incident light was rotated from α=0° (normal to left side, Fig. 4(a)) to α=90° (parallel to left side, Fig. 4(b)). Nonetheless, the appearance of the fluorescence spots completely changed with polarization direction in shape as well as in intensity. Sections along the x-direction through the center of the spots of the left image are presented in Fig. 4(c). Interestingly, the emission intensities between the sub-spots of M1, M2 and M3 decrease within 20-25 nm to the background level indicating that the continuously varying electric field changes its polarity between the sub-spots.

4. Comparison with numerical simulations

In order to determine the orientation of the molecules as well as the different field components at a TA, the measured field patterns are compared to numerical simulations of an aperture in a planar aluminum film of 100 nm thickness. At first, we calculated the electric field distribution $\mathbf{E}(x,y)$ at a distance of 10 nm behind a 50-nm-sized aperture for two different polarization directions of the incident light. The shape of the aperture has been chosen not exactly equilateral for reasons of numerical discretization (cell size is 5.8 x 5.8 x 5.8 nm^3; for more details, see Ref. 10). The excitation intensity I(x,y), which depends on the location (x,y) of the aperture with regard to the probing dipole, is then calculated for many different dipole orientations $\mathbf{p}$ using the relation $I(x,y)=|\mathbf{p}\cdot\mathbf{E}(x,y)|^2$. Note that the simulation does not include fluorescence quenching caused by the metallic end face which can occur for a probe-molecule distance smaller than a few nanometers [1,6].

In Fig. 5(b), a limited number of field maps calculated for several different polar angles θ and azimuth angles φ (cf. Fig. 5(a)) are organized in two panels for two different polarization directions of illumination. In case of a polarization normal to an edge (table on the left), three sub-spots of different intensity generally appear at the aperture. The intensity ratios of the sub-spots strongly vary with dipole orientation so that most orientations create an almost

#9720 - $15.00 USD Received 23 November 2005; revised 15 December 2005; accepted 16 December 2005

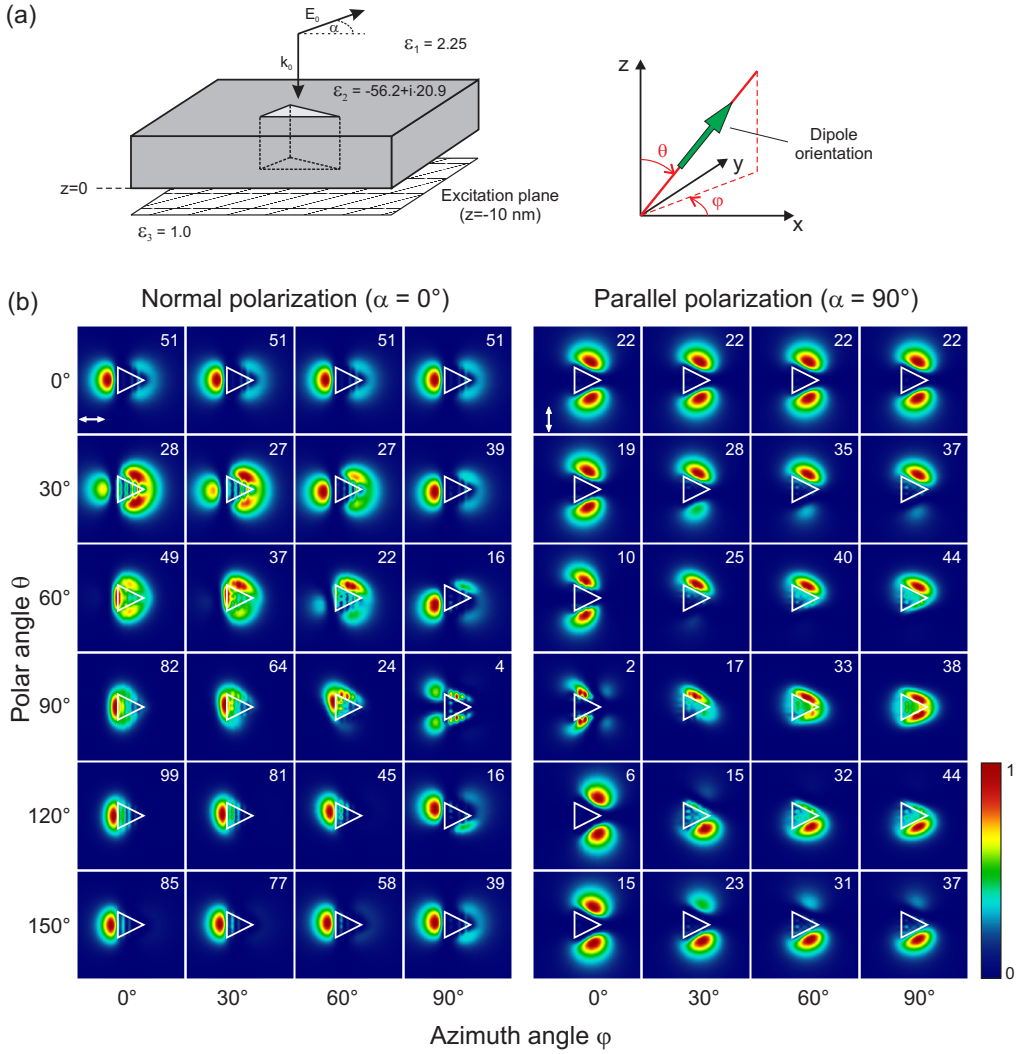

Fig. 5. (a) Numerical model for the simulation of fluorescence patterns caused by single molecules excited through a triangular aperture. The triangular aperture is illuminated at normal incidence with a plane wave which is linearly polarized either perpendicular (α=0°) or parallel (α=90°) to the left aperture edge. The orientation of the absorption dipole moment is represented by the two spherical angles θ and φ. (b) Calculated fluorescence maps for various dipole moment orientations organized in two panels for the two polarization directions α=0° and α=90°. The color scale of each image has been normalized with respect to its maximum intensity value. The number in the upper right corner displays the relative normalization value in percent.

individual pattern. Only for polar angles θ>120°, the patterns are less characteristic because two of the three spots are almost fully suppressed. For this range of polar angles, however, the patterns produced by an illumination polarization direction parallel to an edge (table on the right) are much more sensitive to a change in dipole orientation. Thus for a particular dipole orientation a pair of fluorescence patterns taken from the two panels indeed provides a unique fingerprint.

In order to identify the orientation of a particular molecule, the two measured fluorescence patterns are compared to the calculated field maps of Fig. 5 regarding shape as well as relative intensities of the two maps and the sub-spots. The precision of the orientation determination is then further optimized by gradually changing the angles φ and θ in steps of 1°. As an

#9720 - $15.00 USD Received 23 November 2005; revised 15 December 2005; accepted 16 December 2005

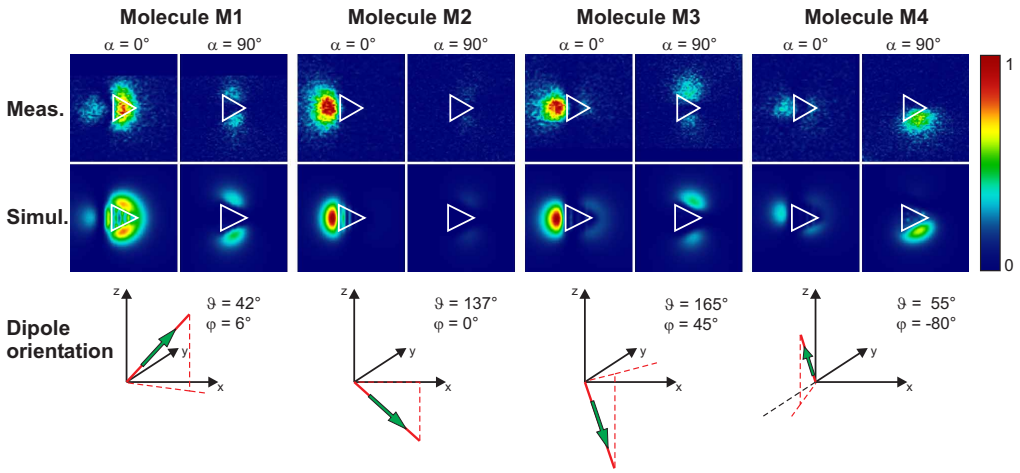

Fig. 6. Comparison of the measured fluorescence patterns (upper row) to the simulated intensity maps I(x,y) (lower row) for the molecules M1 to M4 in Fig. 4(a). For each molecule the maximum intensity of the simulated maps was fitted to the experimental ones without changing the intensity ratio of the two maps for α=0° and α=90°. The deduced dipole moment orientation of each molecule is shown below the images.

example, the measured patterns M1-M4 of Fig. 4 are compared in Fig. 6 to the respective field maps selected in this way.

The agreement between experiment and simulated field maps turned out to be excellent. Not only shape and extension of the patterns but also relative intensities of the fluorescence maxima for both polarizations are reproduced properly. Since molecule-metal interactions were neglected in the simulation, quenching thus seems to have only a minor location-dependent effect on the fluorescence of a fixed molecule in front of a small TA, which is possibly a result of the relatively large probe-molecule distance of >10 nm. Small differences in the near-field distributions of experiment and theory can be attributed to a real molecule-aperture distance deviating from the assumption made in the simulation. In the case of molecule M1, for example, the maximum intensity for α=0° occurs near the center of the aperture whereas in the simulation the maxima are located at the rim. Such a movement of the field maximum to the center is well known to occur with increasing distance to the aperture. The good agreement of theory and experiment together with the high S/N ratio of the data allowed us to determine the orientation angles of a molecule with an uncertainty clearly below 10°. The lateral position of a molecule could be localized with a precision down to a few nanometers (at a pixel time of 20 ms).

Regarding the relative intensities of two differently oriented molecules the agreement between measurement and simulation turned out to be less convincing though the qualitative behavior is similar. Considering the experimental conditions, however, a better agreement could not be expected for at least three reasons: first, the distance of two different molecules to the aperture may differ up to 10 nm (the sample thickness) resulting in a markedly different excitation intensity because the near-field decreases exponentially with distance to the aperture; second, differently oriented molecules have different angular radiation characteristics so that their fluorescence is generally collected with different efficiency (finite numerical aperture of the objective); and third, it is well known, that a metal film near a molecule has a considerable distance- and orientation-dependent influence on the quenching rate and the fluorescence yield of the molecule [1].

From the successful simulation of the experimental fluorescence patterns of single molecules, we can conclude that the simple model of a TA in a planar film is perfectly adequate to describe the near-field optical properties of a real TA probe. A preliminary simulation of a more complex, three-dimensional model of the TA probe confirmed this conclusion, since it produced almost the same results as the simple model. The tetrahedral

#9720 - $15.00 USD Received 23 November 2005; revised 15 December 2005; accepted 16 December 2005

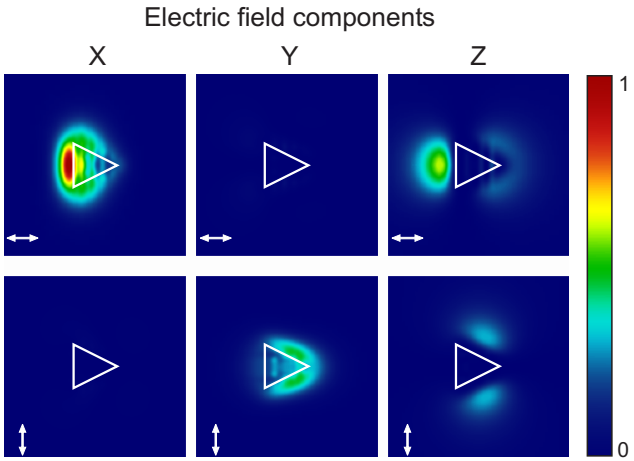

Fig. 7. Square of the electric field components in x-, y- and z-direction at a 50-nm-sized triangular aperture for an illuminating beam polarized normal (upper row) or parallel (lower row) to the left edge. The intensities are normalized to the maximum intensity of the upper left image.

form of the waveguide thus seems to have only a minor influence on the performance of a TA as near-field probe. The spatial distribution of the near-field is mainly shaped by the physical transmission mechanism of electromagnetic fields through the triangular aperture and is much less dependent on the particular way of illumination. In numerical simulations published elsewhere, we could show, for example, that the field distribution is almost independent of the direction of the illuminating beam as long as the film is sufficiently thick and the size of the aperture is much smaller than the wavelength [11]. This is also consistent to our recent result that the general shape of the field pattern at small apertures can be simply deduced from the boundary conditions of electromagnetic fields within the aperture [10].

The experimentally confirmed validity of our numerical model allows us to report the vectorial electric field maps at a real TA probe. These maps are identical with the respective field patterns in Fig. 5 produced by a dipole transition with an orientation in x-direction (θ=90°, φ=0°), y-direction (θ=90°, φ=90°), and z-direction (θ=0°). For a better comparison, the vectorial components of a TA are compiled without normalization in Fig. 7. For both illumination conditions the field component along the direction of the incident electric field is the strongest whereas the respective perpendicular component along the x-axis or y-axis is negligible. In both cases the strength of the z-component is around 60% of the most intense component. Recently, Tanaka and Tanaka discussed the enhanced intensity of the z-component in terms of a surface plasmon polariton excitation on the sidewalls of the aperture [12]. For the field maps resulting from our study, however, it is striking that the intensity maxima are clearly outside the aperture; for the z-components the maxima are even ~25 nm away from the edges. We think that this behavior may be readily explained by considering also the magnetic near-fields at the aperture; related numerical calculations are currently carried out.

5. Conclusion

So far, a triangular nano-aperture was primarily used as ultra-local light source in SNOM measurements. The detailed understanding of the behavior of electromagnetic fields at a triangular aperture described in this paper thus enables a far better interpretation of near-field optical images taken with such a probe. We have demonstrated that the relatively high transmission of triangular nano-apertures together with the enhanced field confinement at only one edge makes it possible to image single fluorescent molecules with high S/N ratio at high optical resolution. Today, most studies employing single molecule detection are based on con-

#9720 - $15.00 USD Received 23 November 2005; revised 15 December 2005; accepted 16 December 2005

focal or wide-field optical microscopy. Owing to the diffraction-limited resolution, however, these approaches require the concentration of fluorescent particles to be largely diluted. In a natural surrounding, e.g. for a biological membrane in its native environment, this is not always possible, so that ultra-sensitive imaging at high optical resolution again becomes desirable [13-15]. Especially in applications where the molecular dipole is free to rotate (e.g., biomolecules in solution), an optical resolution down to 30 nm is readily feasible using a TA probe since on time average the electric field component at the distinguished edge will always be dominant. For molecules with a fixed orientation (e.g., in a lipid membrane) the overall optical spot size may be much less confined so that the optical resolution will be accordingly lower. In this case, however, shape and relative intensities of the measured patterns can be analyzed to figure out the molecular orientation with an accuracy of better than 10°.

Acknowledgments

We thank H. Fuchs for continuous support. The help of F. Pérez-Willard (Laboratorium für Elektronenmikroskopie, University of Karlsruhe) regarding the preparation of FIB-milled apertures is gratefully acknowledged. This work was supported by the Volkswagen foundation within the research program “Physics, chemistry and biology of single molecules”, by the German Science Foundation (FI 608 and NA 382/2), and by the network of excellence “Plasmo-Nano-Devices” of the European community.

#9720 - $15.00 USD Received 23 November 2005; revised 15 December 2005; accepted 16 December 2005